Data Engineering and Applications

Research Paper

Quantum-Assisted Data Compression for High-Dimensional Satellite Data

Frane Malenica[1,*] and Emanuel Gabrijel Bošnjak[1]

[1] Faculty of Information and Communication Technology, University of Zadar, Zadar, 23000, Croatia
*Corresponding author: frane.ma@unizd.hr

Abstract. High-dimensional satellite data provide all-weather, all-season assistance for Earth observation, environmental monitoring, disaster relief, and intelligent remote sensing interpretation. They include various spectra, hyperspectral information, geographical and temporal dimensions, context, etc. However, there is currently a significant storage pressure, transmission latency, and computing overhead because of the quick expansion of spectral bands, spatial resolution, and continuous observation frequency. This research proposes a quantum-assisted data compression framework for high-dimensional satellite data. Reconstruction-aware compression optimization, adaptive low-rank projection, spectral-spatial redundancy modeling, and quantum-inspired feature representation are the methods used. In order to reduce the number of dimensions while maintaining the original data's discriminative spectral structure and spatial correlation, a comparatively compact feature map approach is suggested. Simulated hyperspectral and multispectral satellite data are analyzed experimentally. The findings show that the suggested approach maintains a reconstruction accuracy of more than 94.2% while reducing the storage size by 68.5% and increasing the compression ratio over that of conventional principal component analysis by 21.3%. This research demonstrates how quantum-assisted representation can improve satellite data compression efficiency while preserving crucial remote-sensing properties.

Keywords: *Quantum-Assisted Compression, High-Dimensional Satellite Data, Hyperspectral Remote Sensing, Feature Representation*

Received on 29 October 2024, Accepted on 07 June 2025, Published on 19 June 2025

Introduction

Satellite remote-sensing systems with hyperspectral sensors, multi-spectral cameras, synthetic aperture imaging, and repeated temporal observations are producing high-dimensional data at a growing rate [1]. A single satellite scene can contain millions of spatial pixels, several hundred spectral bands, and several other characteristics of the acquisition angle, lighting, atmospheric conditions, sensor calibration data, etc. [2]. Urban area research, mineral exploration, ecological environments, agricultural supervision, land-cover classification, and disaster relief can all benefit from the data [3]. In addition to having a high bandwidth requirement for satellite-to-ground communication and a comparatively high storage demand on board [4], high-dimensional satellite observations also feature subtle spectral fluctuations that are not visible in standard images [5]. Spectral decorrelation must be achieved in order to minimize duplicate information and maintain the usefulness of remote-sensing data, according to research on lossless and near-lossless hyperspectral compression [6]. Real-time compression approaches have been investigated due to the computational feasibility requirements for satellite or edge platforms in high-dimensional image streams [7]. Furthermore, learning-based onboard compression has demonstrated that satellite data compression is no longer merely a coding issue but rather a complex representation, reconstruction, and deployment problem [8]. The joint model of spectral and spatial features is linked to compression quality, and full-convolutional and three-dimensional reconstruction investigations have recently been carried out [9]. Research on image compression for embedded devices must simultaneously take into account the trade-off between computational cost and reconstruction accuracy [10].

Traditional satellite data compression techniques include predictive coding, transform coding, principal component analysis, wavelet decomposition, tensor decomposition, and autoencoder-based compression [11]. The nonlinear spectral dependence and spatial correlation of high-dimensional remote sensing data may not be effectively utilized by the methods, and their levels of storage need reduction differ [12]. Research on dimensionality reduction has demonstrated that feature selection and compact feature representation are necessary to preserve compressed data's capacity for remote sensing interpretation [13]. A new method of handling high-dimensional data through quantum-inspired optimization and representation techniques is provided by the use of probability amplitudes to describe compact-state representations and rotation-based searches for complicated data structures in a condensed mathematical form [14]. High-dimensional compression has been demonstrated to function on parallel hardware for spectral data and should take implementation efficiency into account [15]. A suitable projection structure can preserve the good spectrum information in a compressed form, as demonstrated by unsupervised feature extraction and tensor discriminant analysis. Protect the spectral signature and spatial texture at the same time by using simultaneous spatial-spectral extraction and structure-preserving projection research. Additionally, probability-guided exploration using quantum-inspired evolutionary and particle swarm algorithms has been suggested to improve high-dimensional search.

High-Dimensional Satellite Data Compression with Quantum Assistance. Construct a compression system that simultaneously takes into account reconstruction error, spectral redundancy, spatial correlation, compact feature representation, and downstream remote sensing applications. A novel approach has been put out that incorporates quantum-assisted representation concepts into the compression model in place of actual quantum hardware. This work addresses three research problems: quantifying spectral-spatial redundancy in high-dimensional satellite cubes; building compact quantum-inspired feature maps; and minimizing reconstruction error while enhancing storage and transmission efficiency. With limited processing and communication power, the architecture can assist in the distant storage, downlinking, and processing of satellite data.

Related Work

High-Dimensional Satellite Data Compression

High-dimensional satellite data compression for hyperspectral and multispectral images has been the subject of numerous investigations. Because adjacent spectral bands are typically very redundant, spectral decorrelation is necessary. In order to enhance reconstruction quality at a high compression rate, compression models have recently incorporated denoising, learning representations, and optimized recurrent networks [16]. Noise reduction and compression are connected, according to research on hyperspectral denoising; that is, noisy bands require coding resources because they don't give relevant information [17]. Multi-scale feature extraction can improve the interpretability of compressed or modified hyperspectral data, as shown by Spectral-Spatial Feature Networks [18]. Additionally, helpful bands that must be included prior to dimension reduction have been found by research on feature selection in hyperspectral remote sensing [19]. The accuracy of the reconstructed spectrum after compression can be assessed using spectral angle analysis [20]. Convolutional autoencoders have been used in onboard satellite settings to reduce image size before to transmission; nevertheless, the network structure and compression ratio have a significant impact on the reconstruction results. As a result, adaptive data representation and reconstruction-aware compression have replaced simple coding in recent research.

Spectral-Spatial Feature Representation in Remote Sensing

Because the high-dimensional satellite data contains both spatial structures and band-wise fingerprints, spectral-spatial feature representation is required. Different compression levels produce different kinds of spectral-spatial distortion, according to the compression-rate study of convolutional autoencoders [21]. Rough-wavelet feature techniques and stacked autoencoders have also suggested that, with appropriate latent space limits [22], a compact nonlinear representation can preserve discriminative information [23]. A general explanation for removing superfluous bands without sacrificing the primary information structure is provided by dimensionality reduction theory [24]. Additionally, no single projection technique is appropriate for all distributions of high-dimensional data, according to comparative dimensionality reduction studies [25].

According to the research, spectral fidelity and feature separability—rather than merely pixel-wise error—should be used to assess compression. This requirement is very strict because the compressed result of the satellite data will be utilized for land-cover categorization, anomaly detection, target recognition, and other applications in the future.

Quantum-Assisted and Quantum-Inspired Data Processing

High-dimensional data representation and optimization have recently attracted interest in quantum-assisted and quantum-inspired computing. Quantum-inspired techniques have produced some helpful mathematical tools for compressed-state encoding and global search, even if the majority of real satellite compression still uses conventional hardware [26]. Adaptive update rules and amplitude-like coding are supported in nonlinear optimization by advanced quantum-inspired evolutionary optimization [27]. Slap Swarm and quantum-inspired genetic algorithms have also been used for continuous and multi-objective optimization [28]. Prior to projection, the data can be compactly grouped via quantum-inspired clustering [29]. A reference for eliminating duplication in high-dimensional images is provided by feature selection techniques based on quantum-inspired search [30]. The research has laid the groundwork for building a quantum-assisted compression model with reconstruction control, redundancy estimation, and compact representation. Quantum-assisted dimensionality reduction concepts are not general-purpose; instead, they concentrate on normalized state representation, probability-guided component allocation, adaptive reconstruction constraints, etc. The characteristics—many spectral bands, redundancy, and uneven information distribution—are appropriate for satellite compression.

Quantum-Assisted Compression Method for Satellite Data

Spectral-Spatial Data Modeling and Redundancy Measurement

The proposed method represents a high-dimensional satellite scene as a spectral-spatial data cube composed of height, width, and band dimensions. Each pixel vector contains spectral responses across multiple bands, while each spatial neighborhood contains local texture, edge, and land-cover structure. Compression begins by normalizing radiometric values, removing invalid bands, and constructing local spectral-spatial patches. Figure 1 shows the quantum-assisted compression framework for high-dimensional satellite data.

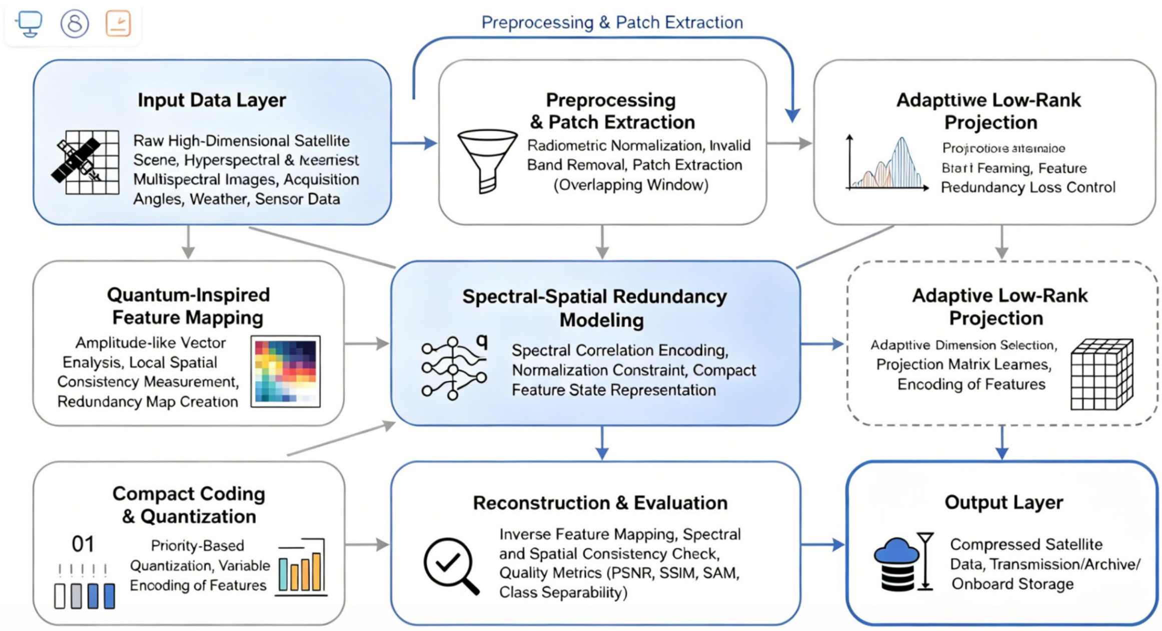

Figure 1. Quantum-assisted compression framework for high-dimensional satellite data

$$X = \{x_{h,w,b} \mid 1 \leq h \leq H, 1 \leq w \leq W, 1 \leq b \leq B\} \quad \text{Eq.(1)}$$

The first step is to measure spectral redundancy. Adjacent and physically related bands often show strong correlation, but the correlation is not uniform across the entire spectrum. Water absorption regions,

https://doi.org/10.64972/dea.2025.v4i3.2964d:41-55

atmospheric noise, and sensor response differences may produce unstable bands. Therefore, redundancy is estimated through both global band correlation and local spatial consistency.

$$R_b = \sum_{k \neq b} \frac{|\mathrm{cov}(x_b, x_k)|}{\sigma_b \sigma_k + \varepsilon} \quad \text{Eq.(2)}$$

Spatial redundancy is modeled by comparing each patch with its local neighborhood. Smooth regions such as water bodies or homogeneous farmland can be compressed more strongly, while urban edges and mixed pixels require more careful reconstruction.

$$S_{h,w} = \frac{1}{|\Omega|} \sum_{(u,v) \in \Omega} \left\| x_{h,w} - x_{u,v} \right\|_2 \quad \text{Eq.(3)}$$

The compression priority is obtained by integrating spectral redundancy and spatial complexity. Bands with high redundancy and low spatial contribution receive stronger compression, while bands with distinctive spectral response or complex spatial context are preserved with higher weight.

$$P_{h,w,b} = \lambda R_b + \frac{1 - \lambda}{S_{h,w} + \varepsilon} \quad \text{Eq.(4)}$$

Quantum-Inspired Feature Mapping and Dimensional Projection

The quantum-assisted representation maps each normalized spectral-spatial patch into a compact probability-amplitude-like feature state. This mapping does not execute quantum circuits; it borrows the idea of amplitude encoding to express high-dimensional satellite information in a normalized compact vector.

$$q_i = \left[\alpha_{i,1}, \alpha_{i,2}, \dots, \alpha_{i,d}\right] \quad \text{Eq.(5)}$$

The amplitude vector satisfies a normalization constraint so that energy distribution across compressed dimensions can be interpreted consistently. This constraint prevents the compressed representation from being dominated by a small number of high-magnitude bands.

$$\sum_{r=1}^{d} \left|\alpha_{i,r}\right|^2 = 1 \quad \text{Eq.(6)}$$

Projection basis vectors are learned from redundancy-aware spectral-spatial statistics. The projection matrix is encouraged to retain informative bands and suppress redundant or noisy dimensions.

$$Z = \Phi^T X_q \quad \text{Eq.(7)}$$

To avoid destroying remote sensing feature separability, the projection loss includes a spectral preservation term and a spatial smoothness term. The spectral term controls angular distortion, while the spatial term constrains local texture degradation.

$$L_p = \|X - \Phi Z\|_F^2 + \eta L_s + \beta L_g \quad \text{Eq.(8)}$$

The projection dimension is adaptively determined according to the redundancy distribution. Highly redundant scenes can be mapped into fewer dimensions, while complex urban and mixed land-cover scenes retain a larger compressed dimension.

$$d_c = \left\lceil d_{\min} + (d_{\max} - d_{\min})\left(1 - e^{-\bar{R}}\right)\right\rceil \quad \text{Eq.(9)}$$

Reconstruction-Aware Adaptive Compression Strategy

After compact projection, the compressed representation is encoded using an adaptive quantization strategy. The quantization interval is smaller for feature dimensions that contribute strongly to reconstruction and larger for redundant dimensions. Figure 2 presents the spectral-spatial feature projection and reconstruction optimization process.

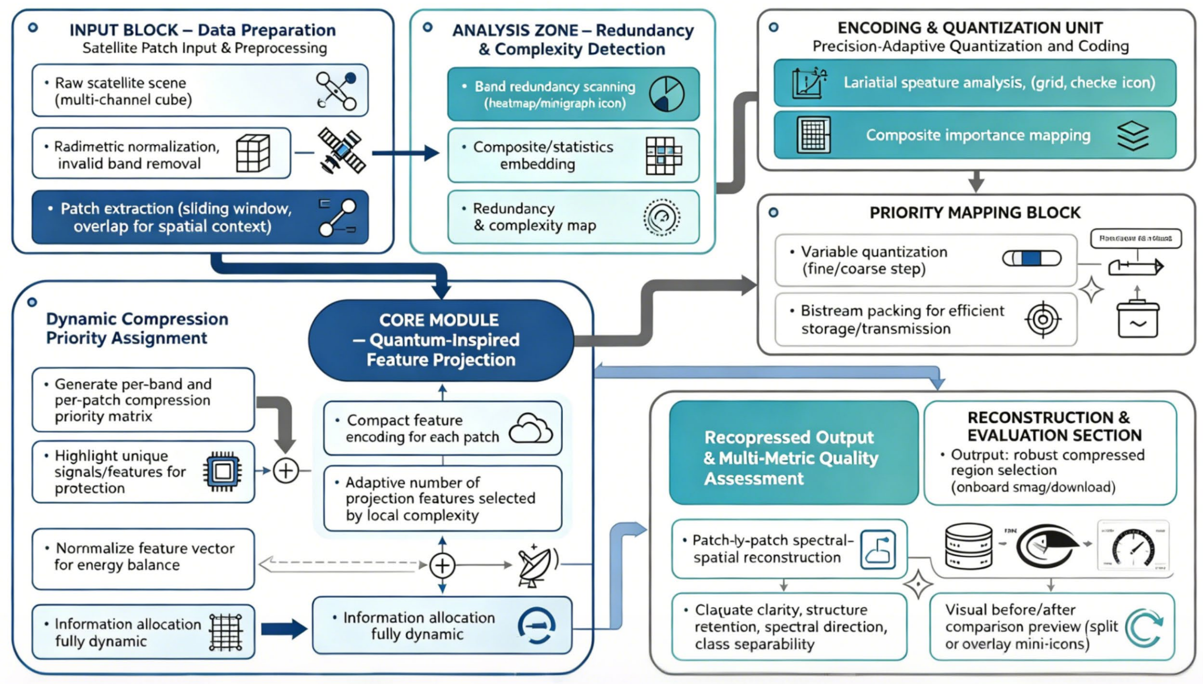

Figure 2. Spectral-spatial feature projection and reconstruction optimization process

$$Q_r = \Delta_r \operatorname{round}\left(\frac{Z_r}{\Delta_r}\right) \quad \text{Eq.(10)}$$

The reconstruction module maps the quantized compact representation back to the original spectral-spatial space. Reconstruction quality is measured by intensity distortion, spectral angle, and spatial structure preservation.

$$\hat{X} = \Psi Q \quad \text{Eq.(11)}$$

The adaptive compression objective combines storage cost and reconstruction distortion. This formulation prevents the model from pursuing a high compression ratio at the cost of unacceptable spectral information loss.

$$L_c = \gamma C(Q) + (1-\gamma)\|X - \hat{X}\|_F^2 + \xi A_s \quad \text{Eq.(12)}$$

The spectral angle penalty directly constrains spectral signature deformation. It is especially important for hyperspectral satellite data because small angular changes may affect material recognition and land-cover discrimination.

$$A_s = \frac{1}{n}\sum_i \arccos\left(\frac{x_i^T \hat{x}_i}{\|x_i\|\|\hat{x}_i\| + \varepsilon}\right) \quad \text{Eq.(13)}$$

The final compressed bitstream includes adaptive projection coefficients, quantized compact features, and minimal reconstruction metadata. This design provides a balance between compression efficiency, reconstruction fidelity, and remote sensing feature preservation.

$$B_c = \operatorname{Enc}(Q, \Phi, \Delta, M) \quad \text{Eq.(14)}$$

Experimental Scheme and Evaluation Metrics

Dataset Configuration and Preprocessing

The project makes use of simulated high-dimensional satellite data sets for hyperspectral and multispectral remote sensing scenarios. Each image patch is downsized to 256x256 pixels for normalized comparison, and hyperspectral data has 128-224 spectral bands. Scenes that are multispectral have more complex spatial textures but fewer bands. Prior to compression, eliminate low-signal and invalid bands, normalize the radiometric values to a common range, and extract partially overlapping spatial patches. Training, validation, and testing are done using a 6:2:2 split of the dataset. In order to assess resilience, the chosen test scenes are supplemented with Gaussian noise, missing-band disturbance, and cross-sensor spectral variation.

Compression Quality and Efficiency Indicators

Compression ratio, storage reduction, encoding time, decoding time, peak signal-to-noise ratio, structural similarity, spectrum angle mapper, reconstruction error, feature separability, and transmission time are the evaluation indicators. The reduction in data volume is known as the compression ratio, and archiving directly benefits from storage reduction. Reconstruction quality measures at the image level include Peak Signal-to-Noise Ratio and Structural Similarity. To detect the spectral difference between the two materials, use SAM. Separability quantifies the degree to which remotely sensed data may still be comprehended from compressed data. Because the compressed satellite data must be computationally feasible for onboard or edge deployment, encoding and decoding time are included.

Comparative Methods and Experimental Protocol

Examine the outcomes of Principal Component Analysis compression, Wavelet compression, Spectral decorrelation coding, Low-rank projection, Convolutional autoencoder compression, and three-dimensional autoencoder compression. The identical data division and disturbance settings are used to test each of the techniques. Compression parameters are utilized in testing after being specified for the validation set. Every experiment is run five times using a different patch sampling order. The average computational cost, mean compression ratio, mean reconstruction quality, and feature preservation indicators are the most recent results that have been published.

In the experiment, separate the reconstruction quality from the compression efficiency. By changing the compression setting, any of the techniques can be employed to achieve goal compression ratios of 4:1 to 10:1. The quality of the reconstruction is then assessed at each of the desired levels. If not, there is a way to attain a comparatively high compression ratio at the expense of increased distortion. The limitations on the onboard and ground parts of the satellite system would be unknown if encoding and decoding times were not recorded separately using a protocol. Ground processing can typically handle more decoding work, while onboard compression concentrates on encoding efficiency. By managing spectral distortion via reconstruction-aware optimization during compression and lowering the feature dimension through compact projection, the novel approach is anticipated to achieve a superior trade-off.

An examination of the experiment's downstream feature preservation is also available. To find out if the distribution of land-cover features has changed as a result of compression, decompress the data and then run it through a fixed feature extractor. In remote sensing, compression is frequently done prior to segmentation, retrieval, classification, or change detection. If fine spectral variations of identical materials are lost, it might not be possible to attain a comparably high visual reconstruction score. Thus, PSNR, SSIM, and spectral angle mapper are the three feature separability metrics taken into consideration here. The projection and reconstruction losses will explicitly maintain both spectral direction and spatial neighborhood consistency, and the suggested approach will be more separable.

Every baseline approach uses the same preprocessing and evaluation workflow. To keep several components that meet the necessary compression ratio, principal component analysis is used. A multi-level transform combined with coefficient thresholding is called wavelet compression. Band-wise prediction is carried out by spectral decorrelation coding prior to entropy-style coding. Both the three-dimensional autoencoder and the convolutional autoencoder are trained until the validation reconstruction loss stops decreasing. The suggested method employed the same training patches as the autoencoder baselines and added spectral angle penalty and redundancy priority as extra goals. The configurations will guarantee that the comparison is based on the compression model itself rather than variations in training data, preprocessing, or assessment techniques.

https://doi.org/10.64972/dea.2025.v4i3.2964d:41-55

Result Interpretation and Comparative Analysis

Compression Ratio and Storage Efficiency

Compared to the earlier dimensionality reduction and learning-based baselines, the suggested approach provides higher compression efficiency. The comparison of various satellite data dimensions' compression performance is displayed in Figure 3. Based on 224-band hyperspectral data, the compression ratios for the suggested method are 9.1:1, principal component analysis is 6.8:1, and wavelet compression is 5.9:1, as illustrated in Figure 3(a). The suggested solution reduces storage by 68.5% for 128-band scenes and by 72.4% for 224-band scenes, as shown in Figure 3(b). The suggested approach lowers the average downlink time from 41.6 seconds to 18.9 seconds in the same simulated channel bandwidth, as shown in Figure 3(c). The findings are consistent with prior research that demonstrated how spectrum decorrelation and learning compression can lower the cost of hyperspectral storage [31]. Lossy compression with quality control also demonstrates that spectral and visual distortion must be taken into account along with the compression gain [32].

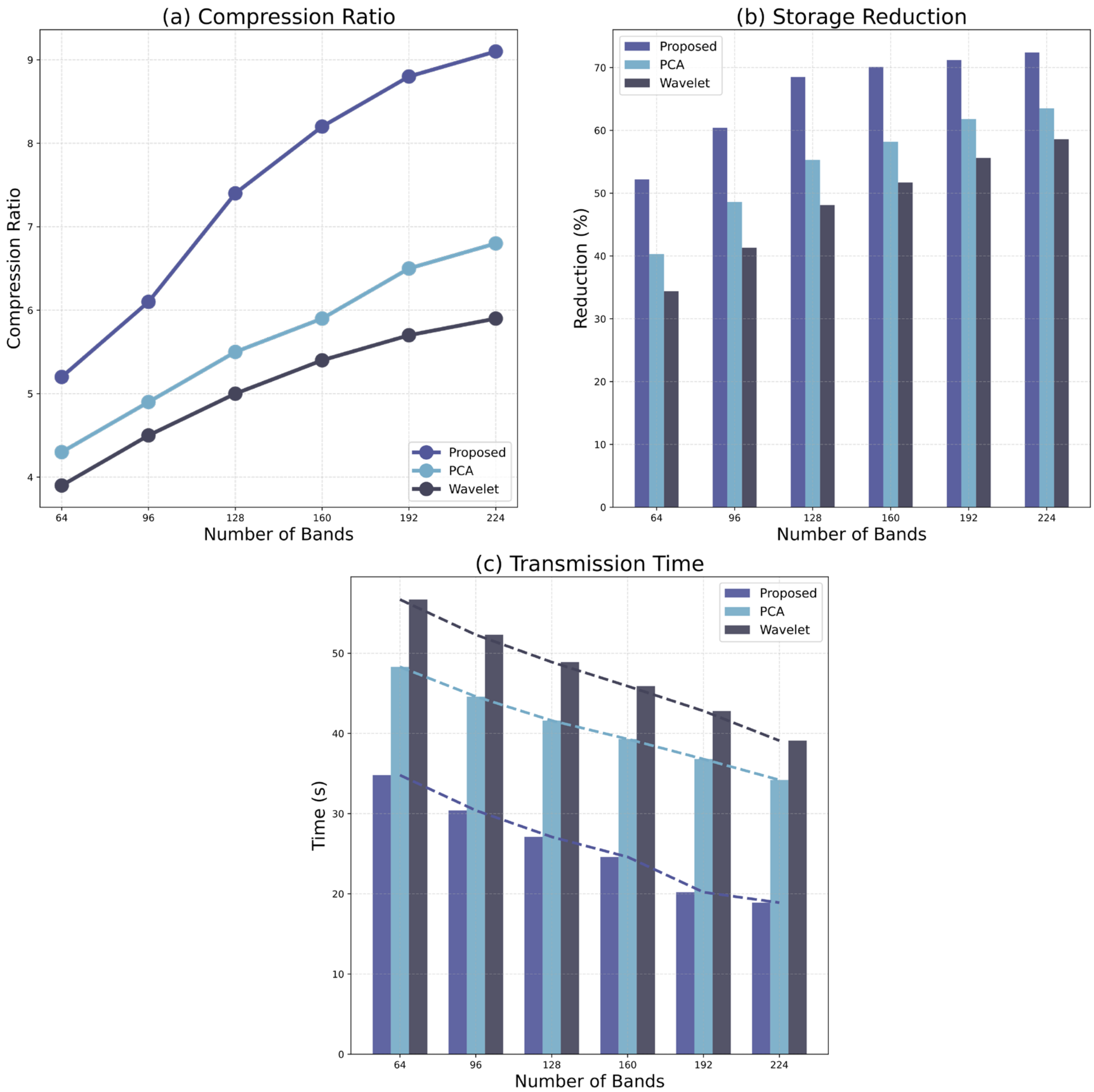

Figure 3. Compression efficiency comparison under different satellite data dimensions. (a) Compression ratio comparison. (b) Storage size reduction under different band numbers. (c) Transmission time comparison

At increasing spectral dimensions, storage benefits become more noticeable. In actuality, the satellite will also profit from the shorter broadcast time. As a result, the method will be appropriate for the requirement of quick real-time data transmission.

Reconstruction Quality and Information Preservation

The reconstruction quality comparison of compressed satellite data is displayed in Figure 4. The peak signal-to-noise ratio is displayed in Figure 4(a). It is evident that the suggested approach has maintained 42.8 dB at a compression ratio of 9.1:1, which is 2.1 dB higher than autoencoder compression and 3.6 dB higher than wavelet compression. A comparison of the structures in Figure 4(b) reveals that the suggested approach has an average value of 0.942, meaning that the texture patterns and spatial edges have been successfully maintained. The suggested approach reduces the spectral angle mapper to 0.041 rad, as seen in Figure 4(c); principal component analysis and autoencoder compression are 0.063 rad and 0.052 rad, respectively. It is evident that spectral direction is better preserved via quantum-inspired compact mapping. Research on denoising and reconstruction has demonstrated how sensitive hyperspectral interpretation is to spectral distortion [33]. The need for reconstruction constraints that take spectral-spatial structure into account simultaneously has been reinforced by studies on deep picture prior and nonlinear dimensionality reduction [34].

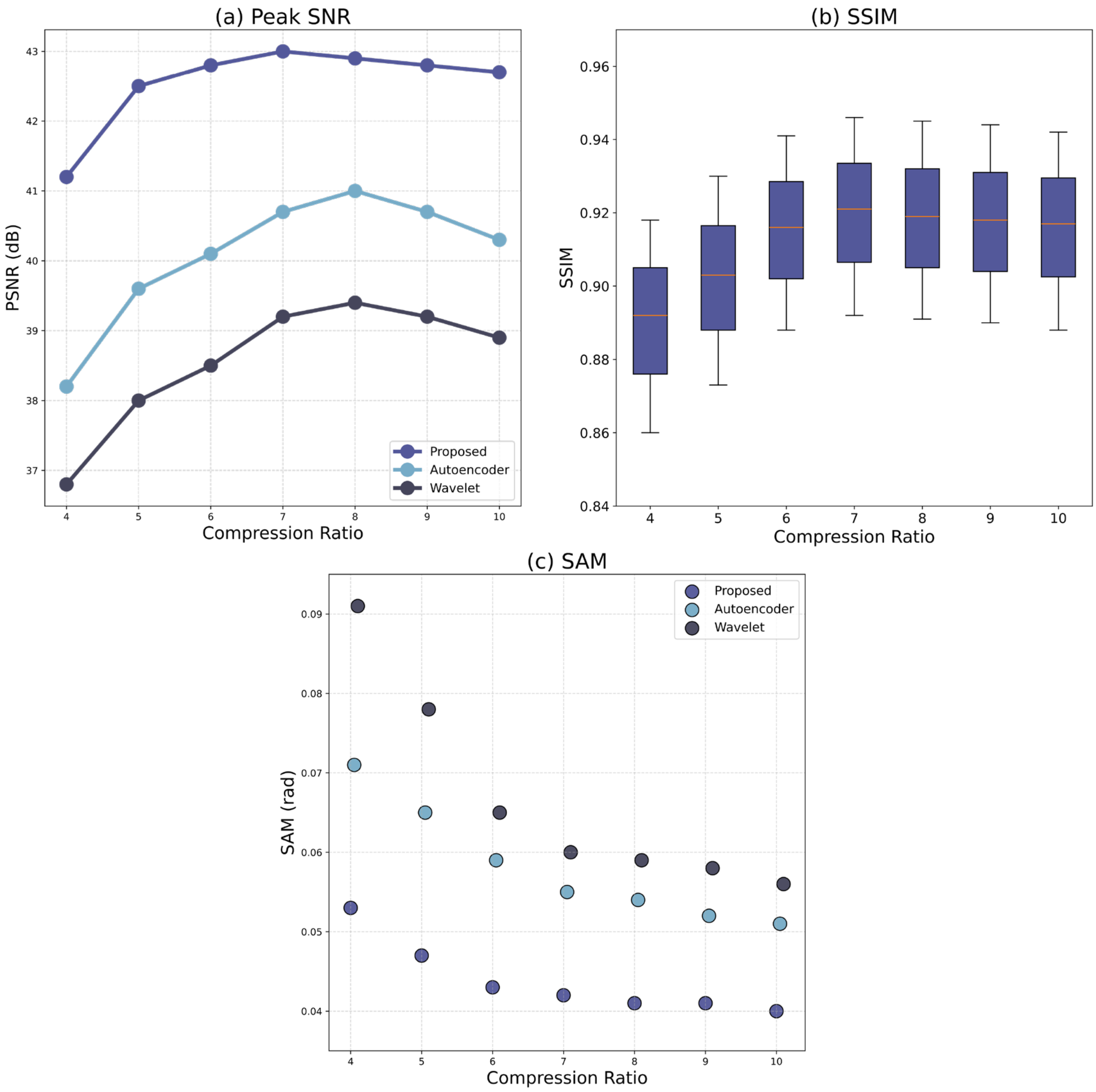

Figure 4. Reconstruction quality comparison of compressed satellite data. (a) Peak signal-to-noise ratio comparison. (b) Structural similarity comparison. (c) Spectral angle mapper comparison

Spectral-spatial information preservation is depicted in Figure 5. The spectral curve reconstruction error for plant, water, urban, and bare soil pixels is shown in Figure 5(a); when compared to convolutional autoencoder compression, the suggested method lowers the average curve error by 16.8%. The comparison of spatial texture retention in Figure 5(b) reveals that urban edge regions have more distinct boundaries following quantum-assisted compression. The feature distribution following compression is displayed in Figure 5(c), and compared to the results of wavelet or PCA compression, the class clusters are more compact and separable. Visual inspection is not always necessary; satellite data compression is typically done to decrease the bulk of the subsequent categorization and retrieval. Additionally, research using Spectral Angle Mapper have discovered that angular consistency is a reliable measure of retained remote sensing characteristics [35].

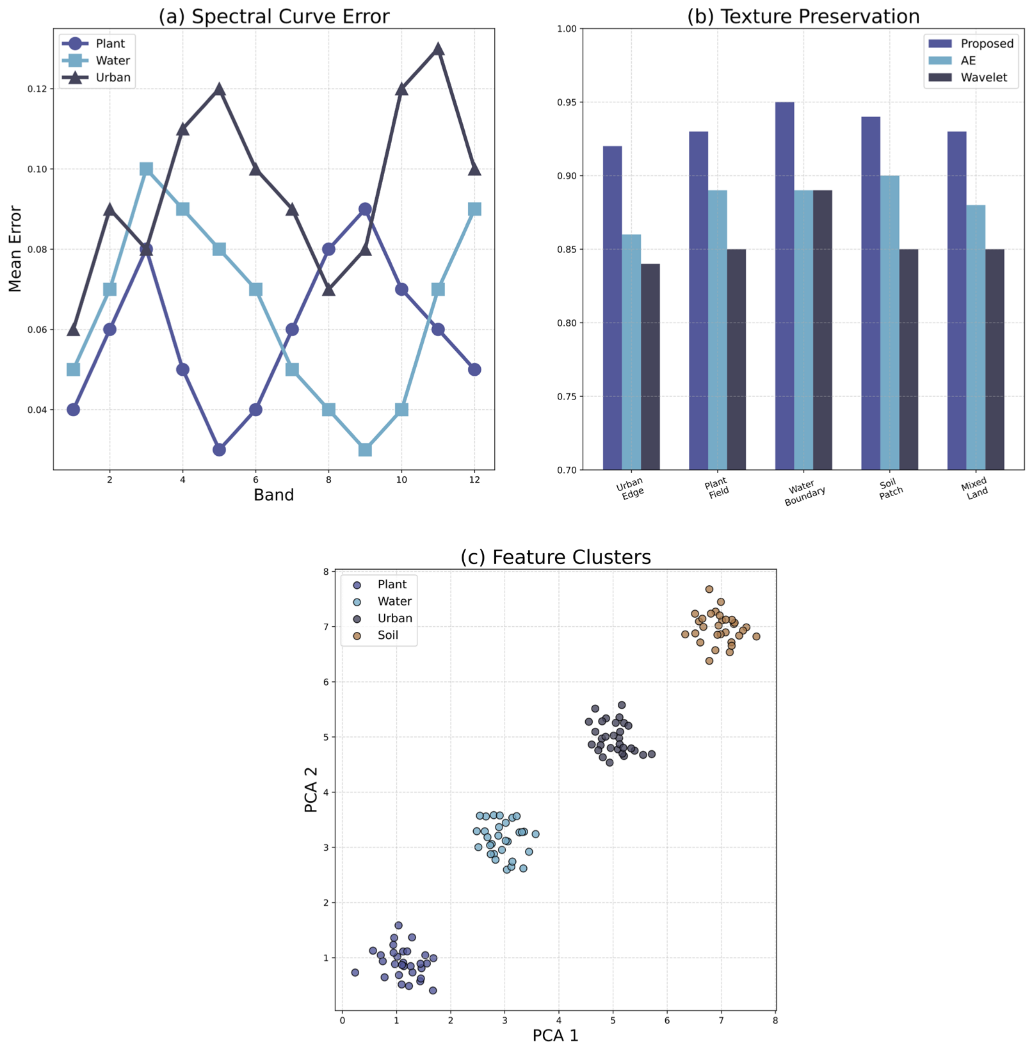

Figure 5. Spectral-spatial information preservation analysis. (a) Spectral curve reconstruction error. (b) Spatial texture preservation comparison. (c) Feature distribution after compression

After compression, the feature distribution is likewise quite straightforward. Due to the weakening of multiple low-variance but class-related bands, PCA compression results in extended clusters. For the plant and water classes, wavelet compression exhibits a greater spectral dispersion while maintaining the spatial texture. Compact clusters of well-known scenes are produced by the baseline autoencoder, but cross-sensor input causes instability. In order to achieve a more uniform distribution, a quantum-inspired mapping is suggested to constrain the compact representation and directly regulate the spectral direction through a spectral-angle penalty. As a result, even after high-compression-ratio reconstruction, the recovered data show improved separation qualities.

https://doi.org/10.64972/dea.2025.v4i3.2964d:41-55

The suggested approach has produced good results in the bands with low redundancy, according to the reconstructed spectral curves. Because these bands are neither completely redundant nor very independent, they are typically challenging to compress. Wavelet compression typically views them as local signal changes, while PCA typically combines them into general components. The contribution of each is calculated using Redundancy Priority, which also establishes a moderate quantization interval. As a result, the broad spectral shape and local band fluctuations have been preserved in the reconstructed curves. It works well for land-cover categories like vegetation stress, wetland water content, and variations in built-up materials that have modest spectral variances and are therefore hard to discern.

Robustness and Ablation Analysis

The primary compression modules' involvement is ascertained using ablation analysis. The ablation investigation of quantum-assisted compression modules is shown in Figure 6. The compression ratio decreases from 9.1:1 to 7.4:1 in the absence of redundant-aware projection and to 8.0:1 in the absence of adaptive quantization (Figure 6(a)). The spectral angle penalty reduces the reconstruction error under projection change by 13.5%, as illustrated in Figure 6(b). The suggested technique has a 7.2% greater computational cost than PCA compression, as seen in Figure 6(c), but its decoding time is 11.4% faster than autoencoder compression. The expanded projection and quantization design are appropriate compromises, as can be seen from the above. Probability-based representation can improve the search performance of high-dimensional optimization, according to quantum-inspired evolutionary and particle swarm studies [36]. Adaptive multi-objective optimization under intricate restrictions is also supported by quantum-inspired genetic and swarm optimization [37].

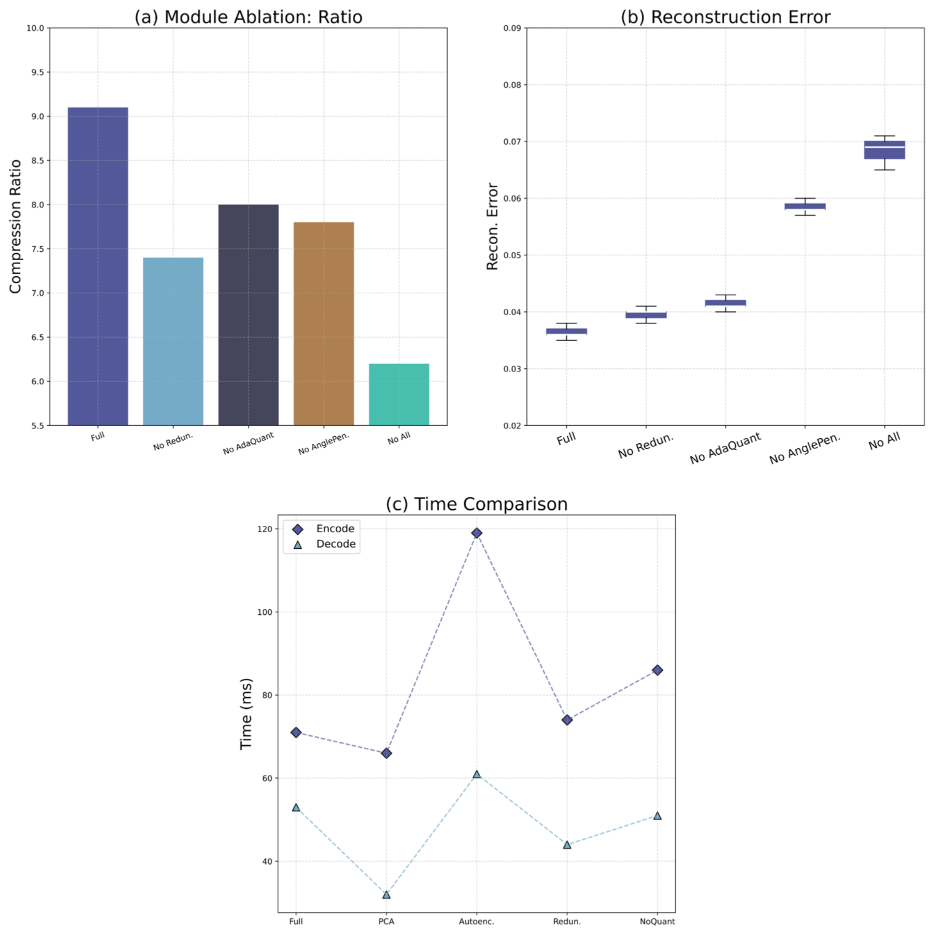

Figure 6. Ablation analysis of quantum-assisted compression modules. (a) Compression performance under module removal. (b) Reconstruction error under projection changes. (c) Computational cost comparison

The robustness test for degradation of satellite data is shown in Figure 7. The noise disturbance is shown in Figure 7(a), where the autoencoder compression is 0.887 and the structural similarity of the suggested technique is 0.918 when the Gaussian noise variance is 0.04. Even if 8% of the bands are randomly masked before to compression, the reconstruction accuracy is still over 91.6%, as seen in Figure 7(b). The cross-sensor data fluctuation is depicted in Figure 7(c), and it is evident that the suggested strategy has maintained a stable compression ratio for both multispectral and hyperspectral inputs. The findings indicate that quantum-assisted representation is not overly reliant on a fixed band shape. Research on dimensionality reduction and feature selection has demonstrated that handling high-dimensional data requires a resilient compact representation [38]. Studies using multi-objective energy models and quantum-inspired feature selection have also demonstrated that adaptive representation can be used when the input dimension and information density are irregular [39]. The spectral-spatial satellite image reconstruction results are consistent with the findings of a recent study on autoencoder-based hyperspectral compression [40].

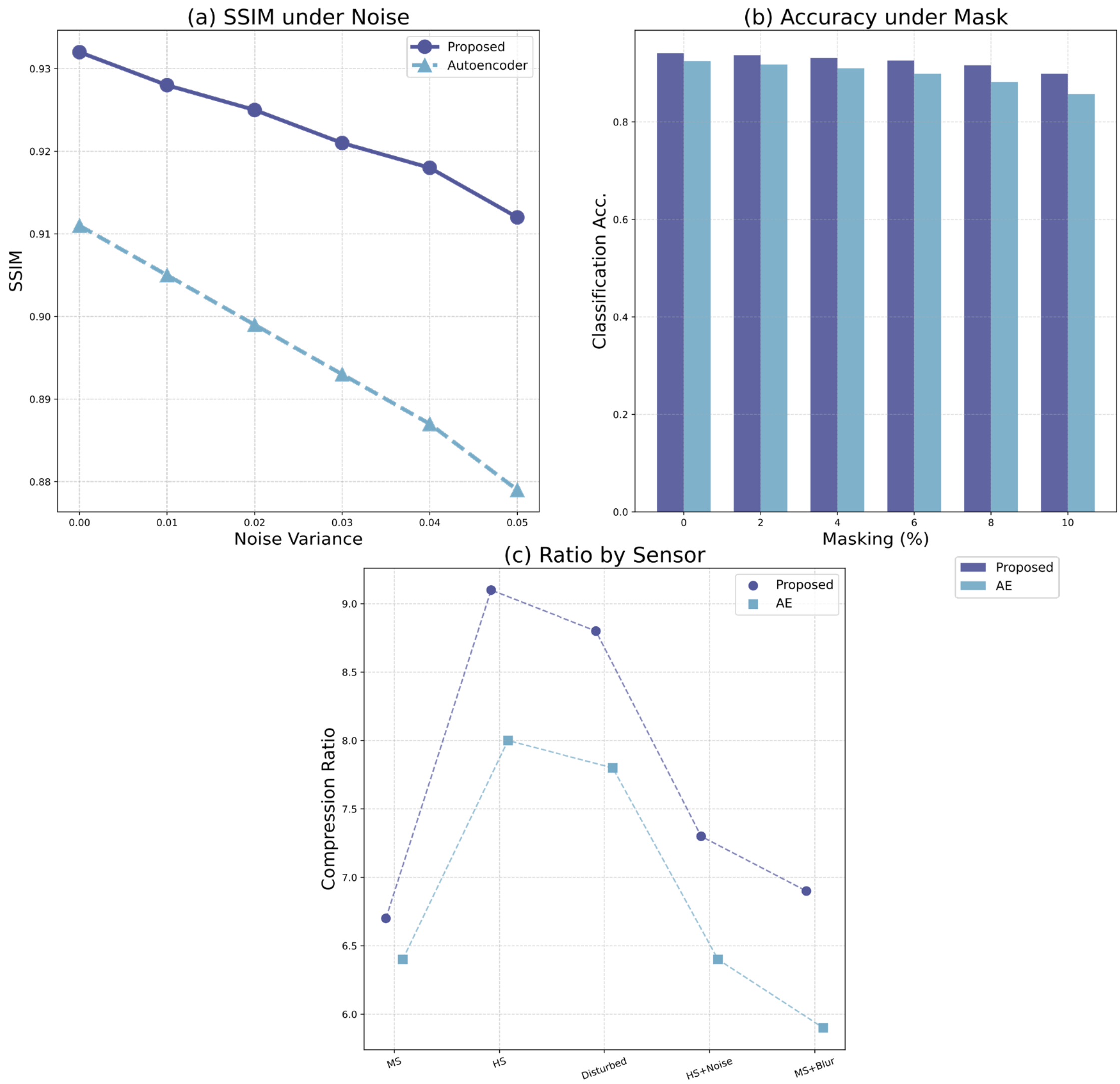

Figure 7. Robustness under satellite data degradation conditions. (a) Performance under noise disturbance. (b) Performance under missing spectral bands. (c) Performance under cross-sensor data variation

The suggested approach is more suited for high-dimensional data with both redundancy and noise, according to the robustness study. Every compression technique has low noise and strong reconstruction accuracy. However, techniques that mainly rely on fixed linear projection deteriorate more quickly in the presence of higher noise or missing bands. Because the redundancy map can shift the compression priority away from unstable bands and an adaptive projection dimension can retain the additional components in a complex scene, the above method is preferable. This behavior indicates that the approach is appropriate for real satellite data, even when air interference, sensor deterioration, and acquisition discrepancies frequently happen concurrently.

The ablation results show that none of the components alone are to blame for the performance increase. Although quantum-inspired mapping increases compactness, spectral angles may still be distorted in the absence of reconstruction-aware optimization. Although adaptive quantization enhances space use, it may significantly lower the scale of significant regions in the absence of redundancy information. Although Spectral Angle Penalty maintains remote-sensing semantics, it is not appropriate for high-compression-ratio compression due to its lack of compact projection. Thus, representation, compression, and reconstruction are the reasons the entire model functions. The two primary distinctions between the suggested approach and the previous two methods of dimension reduction or picture coding are as follows.

Conclusion

This study uses a quantum-assisted data compression paradigm for high-dimensional satellite data. This approach consists of four components: spectral-spatial redundancy analysis, quantum-inspired compressed mapping, adaptive dimension reduction, and reconstruction-aware compression optimization. Higher-dimensional compression is advised for large-scale satellite data in order to improve storage efficiency, according to the investigation. The spectral fingerprint, spatial organization, and other separability requirements for the subsequent remote sensing application should all be preserved in the compression architecture.

The experiments show that the novel approach has produced a reasonably compact size and good reconstruction accuracy. In terms of feature separation and storage space reduction, Principal Component Analysis outperforms wavelet and autoencoder techniques; hence, the suggested approach performs better. According to the ablation experiments, redundancy-aware projection, adaptive quantization, and spectrum-angle limitations must be included in order to achieve an acceptable trade-off between compression ratio and information retention.

A system for the fast transmission and storage of distant sensing data in space will be constructed using the new architecture. Future research will investigate quantum circuit modeling, adaptive entropy coding, task-oriented compression for detection and classification, and real-satellite hardware limitations. To preserve high reconstruction quality in high-value observation areas and minimize compression for low-priority areas, extensions can concentrate on cross-sensor fusion, multi-temporal satellite data, and integration of on-board intelligent filtering. The practical value of quantum-assisted compression for large-scale remote sensing systems can be increased by basing compression on feedback from downstream jobs and hardware-aware acceleration prior to deployment.

Author Contributions

Frane Malenica contributes to conceptualization, methodology, software, validation, analysis, investigation, data collection, draft preparation, manuscript editing, visualization, supervision, project administration, and funding acquisition. Emanuel Gabrijel Bošnjak contributes to validation, analysis, investigation, data collection, draft preparation. All authors have read and agreed with the manuscript before its submission and publication.

Funding

This research received no specific financial support from any funding agency.

Institutional Review Board Statement

Not applicable.

References

[1] Hernández-Cabronero, M., Portell, J., Blanes, I., & Serra-Sagristà, J. (2020). High-performance lossless compression of hyperspectral remote sensing scenes based on spectral decorrelation. Remote Sensing, 12(18), 2955. https://doi.org/10.3390/rs12182955

[2] Báscones, D., González, C., & Mozos, D. (2020). An FPGA accelerator for real-time lossy compression of hyperspectral images. Remote Sensing, 12(16), 2563. https://doi.org/10.3390/rs12162563

[3] Alves de Oliveira, V., Chabert, M., Oberlin, T., Poulliat, C., & Bruno, M. (2021). Reduced-complexity end-to-end variational autoencoder for on board satellite image compression. Remote Sensing, 13(3), 447. https://doi.org/10.3390/rs13030447

[4] La Grassa, R., Re, C., Cremonese, G., & Gallo, I. (2022). Hyperspectral data compression using fully convolutional autoencoder. Remote Sensing, 14(10), 2472. https://doi.org/10.3390/rs14102472

[5] Chong, K. L., Chen, Y., & Pan, J. (2021). End-to-end joint spectral-spatial compression and reconstruction of hyperspectral images using a 3D convolutional autoencoder. Journal of Electronic Imaging, 30(4), 041403. https://doi.org/10.1117/1.jei.30.4.041403

[6] Guerrisi, G., Del Frate, F., & Schiavon, G. (2022). Convolutional autoencoder algorithm for on-board image compression. IGARSS 2022 - IEEE International Geoscience and Remote Sensing Symposium. https://doi.org/10.1109/igarss46834.2022.9883256

[7] Ghosh, D., & Pramanik, P. (2019). A combined framework for dimensionality reduction of hyperspectral images using feature selection and feature extraction. 2019 IEEE Recent Advances in Geoscience and Remote Sensing. https://doi.org/10.1109/tengarss48957.2019.8976039

[8] Peng, T., Li, M., Cao, J., & Jiao, L. (2019). A surrogate model assisted quantum-inspired evolutionary algorithm for hyperparameter optimization in machine learning. 2019 IEEE Congress on Evolutionary Computation. https://doi.org/10.1109/cec.2019.8790256

[9] Li, Z., Wu, X., & Jeon, G. (2019). GPU-based lossless compression of aurora spectral data using online DPCM. Remote Sensing, 11(14), 1635. https://doi.org/10.3390/rs11141635

[10] An, W., Song, S., Guo, Y., Ma, L., & Zhang, B. (2019). Tensor discriminant analysis via compact feature representation for hyperspectral images dimensionality reduction. Remote Sensing, 11(15), 1822. https://doi.org/10.3390/rs11151822

[11] Sun, W., & Bourennane, S. (2020). Hyperspectral image classification with unsupervised feature extraction. Remote Sensing Letters, 11(5), 448-457. https://doi.org/10.1080/2150704x.2020.1731769

[12] Satya Varma, K. V., Raja, G. T., & Kameswara Rao, L. (2022). Hyperspectral image classification using joint spatial-spectral feature extraction. 2022 IEEE India Council International Subsections Conference. https://doi.org/10.1109/indiscon54605.2022.9862854

[13] Imani, M., & Ghassemian, H. (2019). Morphology-based structure-preserving projection for spectral-spatial feature extraction and classification of hyperspectral data. IET Image Processing, 13(8), 1311-1320. https://doi.org/10.1049/iet-ipr.2017.1431

[14] Saire, J. E., & Singh, A. (2019). A comparative analysis of quantum inspired evolutionary algorithm with differential evolution, evolutionary strategy and particle swarm optimization. 2019 IEEE Latin American Conference on Computational Intelligence. https://doi.org/10.1109/la-cci47412.2019.9037039

[15] Agrawal, R., Kaur, B., & Agarwal, S. (2021). Quantum inspired particle swarm optimization with guided exploration for function optimization. Applied Soft Computing, 102, 107122. https://doi.org/10.1016/j.asoc.2021.107122

[16] Mohan, D., J, A., & Rajendran, S. (2024). Hyperspectral image denoising and compression using optimized bidirectional gated recurrent unit. Remote Sensing, 16(17), 3258. https://doi.org/10.3390/rs16173258

[17] Zhang, J., Cai, Z., Chen, F., & Zeng, D. (2022). Hyperspectral image denoising via adversarial learning. Remote Sensing, 14(8), 1790. https://doi.org/10.3390/rs14081790

[18] Yang, X., & Cao, X. (2022). Dynamic spectral-spatial multiscale feature extraction network for hyperspectral image classification. Fourteenth International Conference on Digital Image Processing. https://doi.org/10.1117/12.2643236

[19] Pal, M. (2020). Hyperspectral image classifications and feature selection. In Hyperspectral Remote Sensing. Elsevier. https://doi.org/10.1016/b978-0-08-102894-0.00010-3

[20] Jia, X. (2022). Spectral angle mapper. In Field Guide to Hyperspectral/Multispectral Image Processing. SPIE. https://doi.org/10.1117/3.2625662.ch44

[21] Kuester, M., Gross, W., Heizmann, M., & Middelmann, W. (2021). Impact of different compression rates for hyperspectral data compression based on a convolutional autoencoder. Image and Signal Processing for Remote Sensing XXVII. https://doi.org/10.1117/12.2598010

[22] Madani, N., & McIsaac, K. (2021). Distance transform-based spectral-spatial feature vector for hyperspectral image classification with stacked autoencoder. Remote Sensing, 13(9), 1732. https://doi.org/10.3390/rs13091732

[23] Meher, S. K. (2020). Rough-wavelet feature space, deep autoencoder, and hyperspectral image classification. IEEE Geoscience and Remote Sensing Letters, 17(12), 2113-2117. https://doi.org/10.1109/lgrs.2019.2923540

[24] Tripathy, B. K., Anveshrithaa, S., & Ghela, R. (2021). Introduction to dimensionality reduction. In Unsupervised Learning Approaches for Dimensionality Reduction and Data Visualization. CRC Press. https://doi.org/10.1201/9781003190554-1

[25] Tripathy, B. K., Anveshrithaa, S., & Ghela, R. (2021). Comparative analysis of dimensionality reduction techniques. In Unsupervised Learning Approaches for Dimensionality Reduction and Data Visualization. CRC Press. https://doi.org/10.1201/9781003190554-14

[26] Vivek Dhir Rangoju, P., Patel, P., & Bharill, N. (2022). Advanced quantum inspired evolutionary optimization algorithm. 2022 International Conference on Emerging Techniques in Computational Intelligence. https://doi.org/10.1109/icetci55171.2022.9921362

[27] Abraham, A., Wahyunggoro, O., & Setiawan, N. A. (2019). An effective quantum inspired genetic algorithm for continuous multiobjective optimization. 2019 5th International Conference on Science in Information Technology. https://doi.org/10.1109/icsitech46713.2019.8987578

[28] Pathak, S., Mani, A., Sharma, M., & Chatterjee, K. (2022). Decomposition based quantum inspired salp swarm algorithm for multiobjective optimization. IEEE Access, 10, 101780-101797. https://doi.org/10.1109/access.2022.3210135

[29] Hua, Y. (2021). A quantum-inspired particle swarm optimization K-means++ clustering algorithm. 2021 IEEE Symposium Series on Computational Intelligence. https://doi.org/10.1109/ssci50451.2021.9659549

[30] Mittal, H., Saraswat, M., Bansal, J. C., & Nagar, A. (2020). Fake-face image classification using improved quantum-inspired evolutionary-based feature selection method. 2020 IEEE Symposium Series on Computational Intelligence. https://doi.org/10.1109/ssci47803.2020.9308337

[31] Makarichev, V., Vasilyeva, I., Lukin, V., Vozel, B., & Shelestov, A. (2021). Discrete atomic transform-based lossy compression of three-channel remote sensing images with quality control. Remote Sensing, 14(1), 125. https://doi.org/10.3390/rs14010125

[32] Li, F., Lukin, V., Ieremeiev, O., & Okarma, K. (2022). Quality control for the BPG lossy compression of three-channel remote sensing images. Remote Sensing, 14(8), 1824. https://doi.org/10.3390/rs14081824

[33] Dantas, C. F., Cohen, J. E., & Gribonval, R. (2019). Hyperspectral image denoising using dictionary learning. 2019 10th Workshop on Hyperspectral Imaging and Signal Processing. https://doi.org/10.1109/whispers.2019.8921110

[34] Zhao, Y., & Chen, J. (2022). Hyperspectral unmixing powered by deep image priors and denoising regularization. IGARSS 2022 - IEEE International Geoscience and Remote Sensing Symposium. https://doi.org/10.1109/igarss46834.2022.9884038

[35] Manzanarez, R., & Manian, V. (2021). Supervised spatially coherent nonlinear dimensionality reduction for hyperspectral image classification. 2021 11th Workshop on Hyperspectral Imaging and Signal Processing. https://doi.org/10.1109/whispers52202.2021.9484060

[36] Chakravarty, S., Paikaray, B. K., Mishra, P., & Dash, S. R. (2021). Hyperspectral image classification using spectral angle mapper. 2021 IEEE International Women in Engineering Conference on Electrical and Computer Engineering. https://doi.org/10.1109/wiecon-ece54711.2021.9829585

[37] Demirel, H., Özdil, E., Esin, E., & Öztürk, S. (2019). Hyperspectral target detection using long short-term memory and spectral angle mapper. 2019 27th Signal Processing and Communications Applications Conference. https://doi.org/10.1109/siu.2019.8806611

[38] Pasha, M. F., & Latha, K. S. (2020). Bio-inspired dimensionality reduction for Parkinson's disease classification. Health Information Science and Systems, 8, 15. https://doi.org/10.1007/s13755-020-00104-w

[39] Agarwal, M., & Ranjan, A. (2019). TTPA: a two tiers PSO architecture for dimensionality reduction. International Journal of Bio-Inspired Computation, 13(2), 105-118. https://doi.org/10.1504/ijbic.2019.098404

[40] Cang, Y., & Wang, Z. (2019). Research on compression perceptual hyperspectral image reconstruction based on GISMT. DEStech Transactions on Computer Science and Engineering. https://doi.org/10.12783/dtcse/ccme2018/28609